

## A NEWLY AVAILABLE SCALE-MODELLING FACILITY

A. R. BAYS<sup>1</sup> AND K. DUCKWORTH<sup>1</sup>

### ABSTRACT

A laboratory system for scale modelling of electromagnetic prospecting devices has been developed. It employs a large tank of electrolyte to simulate conductive environments. Digital treatment of signals permits operation in frequency or time domain. Examples of the application of the system to modelling the Turam exploration system are described.

These examples show a case of anomaly enhancement and unusual displacement due to current gathering, a case of the influence of a conductive overburden that is unlike previously reported cases, and a case involving an unconventional operating procedure that appears to provide advantages in the search for deep targets in conductive environments.

### INTRODUCTION

A project aimed at developing a scale-modelling facility that could simulate the behaviour of a wide range of exploration systems was started in the Department of Geology and Geophysics at The University of Calgary in 1979. Because of the interests of the sponsors of the project, the facility was developed initially as an electromagnetic (EM) modelling system. It was clear from the outset, however, that if a signal acquisition and processing system could be developed that was capable of handling the severe requirements for signal processing in an EM model (*e.g.*, treatment of frequencies up to 500 kHz with measurement accuracy of  $\pm 0.2\%$  in amplitude and  $\pm 0.2^\circ$  phase), that system could then be readily adapted to the requirements of seismic scale modelling.

At this time the system is operative as an EM model and its adaptation to seismic modelling and induced-polarization modelling is proceeding. The purpose of the present discussion is to describe the facility and illustrate its capabilities in the study of electromagnetic exploration devices. It is intended that a later paper will be devoted to the application of the facility to seismic modelling.

We believe that the range of frequencies available, allied to the signal-processing methods employed and

the flexibility for simulating conductive environments, allows this system to equal or exceed the performance of other modelling facilities throughout the world.

### THE OPERATING SYSTEM

The system has been designed to allow computer control of all aspects of its operation other than the setting up of the models to be tested. Software development was aimed at allowing the system to be operated by individuals who are only interested in the end product and its geological significance. An intimate knowledge of the functioning principles of the system is not required. The operator is provided with control over the selection of the number of traverses and their position; thereafter the computer controls the operation of the model. A complete list of all the control options that are available has been provided by Bays (1982).

### FEATURES OF THE MODELLING SYSTEM

The modelling of geologic conditions in which the environment is conductive requires that the model simulate that conductive volume, and this is most easily achieved by the use of a large tank of sodium chloride solution. This tank is shown in Figure 1, along with the beam that carries the various transmitting and receiving devices being modelled.

As electromagnetic devices would respond strongly to a metal tank, the tank must be of nonconductive material, and in this case wooden construction with PVC liner was used. The dimensions of the tank are 6 m  $\times$  3 m  $\times$  1.2 m so that, when filled, it holds 21.6 tonnes of solution. This large volume was necessary to permit the modelling of large transmitting antennas of the fixed-loop type while minimizing effects due to the walls of the tank.

The overhead beam that supports and moves the device to be modelled (Fig. 2), is of wooden box-type construction. It was deliberately made much stronger

<sup>1</sup> Department of Geology and Geophysics, The University of Calgary, Calgary, Alberta

The funding for the construction of this modelling facility was provided by donations from Hudson's Bay Oil and Gas Co. Ltd. and AGIP Canada Ltd.

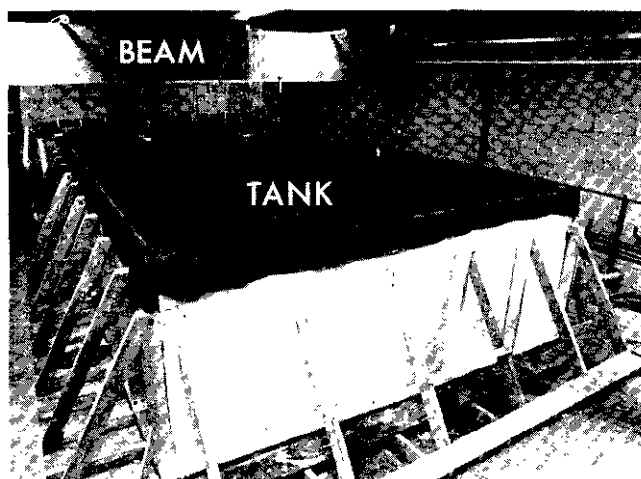


Fig. 1. Over-all view of the scale-modelling facility. The transmitting loop is located at the far end of the tank.

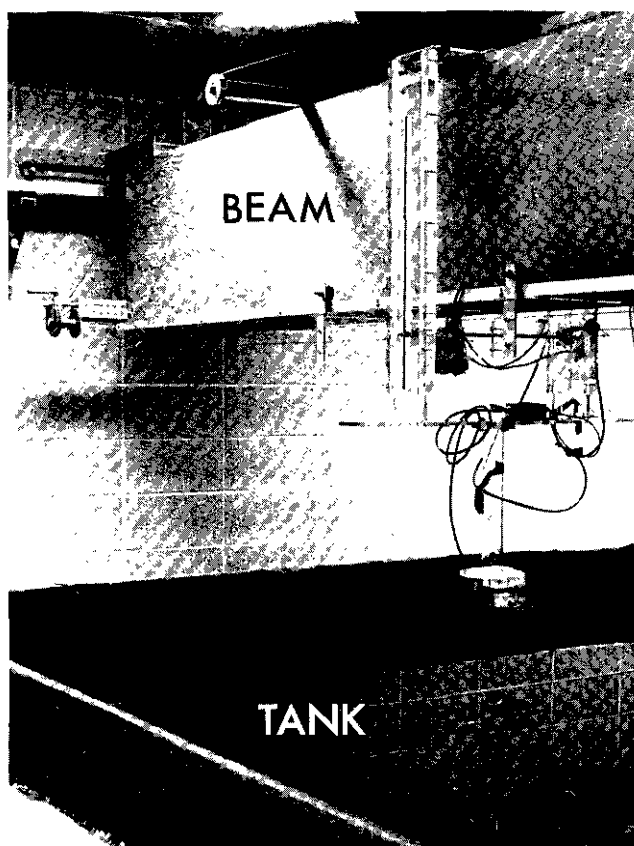


Fig. 2. View of one end of the supporting beam showing the (Y axis) carriage assembly. One of the drive motors for the X axis is visible in the upper left.

than necessary for the support of the model carriage shown in Figure 2, because of its secondary role in lifting models out of the tank when modifications are to be made. As a result of this great rigidity, the model carriage causes negligible sag as it traverses the length of the beam. Three components of positional control for

the model carriage are available. The movement along the room (X axis) is achieved by moving the whole beam under computer control by using stepping motors at both ends. The motors drive flanged wheels which ride on metal rails mounted on the walls of the tank room. The full range of movement is 8 m, so that sensing devices can be placed anywhere within the 6-m length of the tank, or models can be removed from the tank completely. Movement across the room (Y axis) is achieved by driving the model carriage along rails attached to the beam. A single stepping motor provides control in this direction over a range of 4 m. Vertical movement of the carriage (Z axis) is again under computer control, thus permitting simulation of the traversing of sensing devices at various heights above the model, or simulation of downhole surveys using subsurface sensors. The system refers to microswitch-controlled zero points on the rail system at the beginning of each experiment, and can position the model carriage anywhere within the tank to within  $\pm 0.5$  mm.

All the associated electronic equipment, except for one preamplifier, is installed in the room adjacent to that containing the tank. This separation is necessary because the atmosphere of the tank room may become corrosive to electronic equipment if highly concentrated salt solutions are used in the tank.

The system was designed from the outset to take advantage of digital methods in the acquisition and processing of signals. It can thus simulate both the discrete frequency (or continuous wave) devices and the so-called transient EM (or wide band) devices, which require the signal averaging permitted by digital methods in order to obtain usable signal-to-noise ratios. The initial work on the system has concentrated on the devices that employ discrete-frequency, continuous-wave signals, where it was found that digital processing also provides significant benefits in signal handling.

#### TURAM MODELLING

The initial development of the model was directed toward a study of the Turam exploration system, in which a large rectangular loop of wire lying on the ground forms the transmitter. The conventional arrangement of such a transmitter with respect to the trend of an expected target and the traverse lines used by the receiver are shown in Figure 4. The Turam device employs two receiver coils which move at fixed spacing along the traverse, with measurements being made of two field parameters — the ratio of the amplitudes of the signals detected by the two coils (called the Field Strength Ratio or FSR), and the phase difference (PD) between those signals. In presenting the data, the FSR values are normalized with respect to the nonanomalous primary field as described by Bosschart (1964), so that data are normally presented in the form of this normalized or Reduced Field Strength Ratio (RFSR) while PD is presented without alteration. This differential type of receiv-

ing system provides several advantages in the full-scale system, among them being elimination of the need for a phase link to the transmitter, immunity from spurious readings due to variations in transmitter output, and automatic rejection of noise which occurs in both coils with the same amplitude and phase. In the model, provision of a phase link and accurate control of the transmitter are easily achieved, while noise can be dealt with by means of signal averaging, so that only a single detector coil need be used. The absolute amplitude and phase data recorded by such a single-coil receiver are converted to the form normally provided by the Turam device with only a minor amount of additional data manipulation.

The model transmitter loop used in the simulation of the Turam device is shown in Figure 1, while the single sensing coil is shown in Figure 3. The mounting for the sensing coil allows it to be rotated to any desired orientation so that, if required, the coil can be set in sequence to measure the vertical and then two horizontal components of the field over the model. At present the orientation of the coil is set manually, but this function can be handled by computer if a large number of changes of coil orientation becomes necessary.

#### DATA ACQUISITION AND PROCESSING

Signals detected by the sensing coil shown in Figure 3 are preamplified at a point as close as possible to the coil. This avoids amplification of any spurious signals that may be induced into the long lines needed to carry the signals into the next room, and also isolates the cable capacitance from the tuning circuit for the coil. The preamplified signal is further amplified and then digitized by a Nicolet Explorer III digital oscilloscope that also provides a visual monitor of the signal. The minimum digitizing interval provided by the oscilloscope is 50 ns. Thus frequencies up to 5 MHz could be treated but at this time we have not found a need to work above 500 kHz.

A single example of the signal (consisting of a data set of up to 4000 point voltage values) does not provide the required level of measurement precision, so that some signal processing is necessary, which in this system is achieved by having the oscilloscope transfer each data set to an Apple II + Microcomputer. Once the processing parameters have been specified, the process of acquiring and transferring the data is entirely under the control of the computer.

A correlation process is used in extracting phase data from the stacked signals. Amplitude data can also be obtained by this process, but a simple integration process was found to measure amplitudes faster and more accurately.

As a result of this processing, it has been found possible to measure phase at up to 400 kHz to within  $\pm 0.2^\circ$  (*i.e.*,  $\pm 1.5$  ns) and amplitudes to within  $\pm 0.2\%$ . A notable feature of the processing is its ability to retrieve

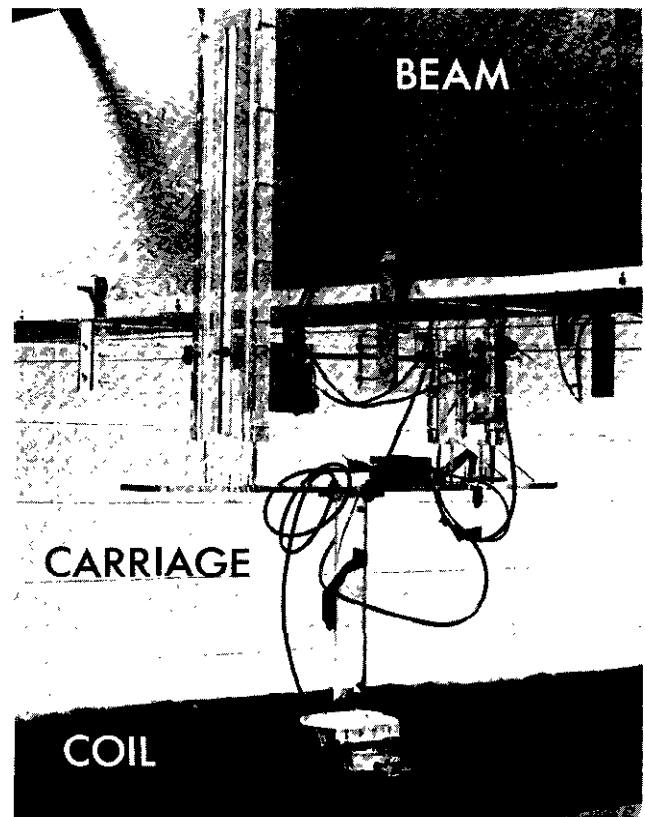


Fig. 3. Close-up view of the Y-axis carriage showing the vertical positioning apparatus and adjustable coil mount.

signals that, due to noise, are unidentifiable on the visual monitor.

#### SCALING CONSIDERATIONS

When modelling EM devices, it is necessary to scale not only the linear dimensions of the device and the geologic model, but also the conductivities and signal frequencies used, because the reciprocal of the square root of the product of conductivity frequency and magnetic permeability has the dimensions of length. The physical reality is seen in the concept of skin depth  $\delta$ , in which

$$\delta = \{2/\sigma\mu\omega\}^{1/2} \text{ m}$$

where  $\sigma$  is conductivity in Siemens/m

$\mu$  is magnetic permeability (normally  $4\pi \times 10^{-7}$ )

$\omega$  is angular frequency (*i.e.*,  $\omega = 2\pi f$ )

$\delta$  is the depth into a conductive medium at which an electromagnetic wave will have been attenuated to  $1/e$  of its original amplitude on entering the conductive medium.

Given two physical systems with linear dimensions  $L_1$  and  $L_2$  having skin depths  $\delta_1$  and  $\delta_2$ , the two systems will be electromagnetically identical if

$$\frac{L_1}{\delta_1} = \frac{L_2}{\delta_2}$$

which leads to

$$L_1^2 \sigma_1 \omega_1 \mu_1 = L_2^2 \sigma_2 \omega_2 \mu_2$$

This expression has been derived in a variety of ways by different authors, but the most thorough discussion was provided by Sinclair (1948).

The magnetic permeability of most materials falls within a narrow range, so that it is difficult to change permeability between the two systems. As a consequence, it is usual to let  $\mu_1 = \mu_2$ , and we are left with only  $\sigma$  and  $\omega$  as the means of adjusting one of these systems to exactly match the other.

Controlled changes in the conductivity of 21.6 tonnes of solution are not easily achieved; consequently, the tank conductivity was fixed at 12.1 S/m and not varied thereafter. This left  $\omega$  as the sole variable by which similitude could be maintained. In the scaling relationship, any three of the parameter scaling factors can be arbitrarily nominated, which thus requires the fourth scaling factor to adopt a value that allows

$$\frac{L_1^2 \sigma_1 \omega_1 \mu_1}{L_2^2 \sigma_2 \omega_2 \mu_2} = 1$$

For example, in the modelling described in the later section we set the linear scaling factor at  $L_1/L_2 = 1000/1$  (i.e., the full-scale system would be 1000 times bigger than the model); we also set  $\omega_1/\omega_2 = 1/200$  and, as mentioned earlier,  $\mu_1/\mu_2 = 1$ . Thus

$$10^6 \cdot \sigma_1 / \sigma_2 \cdot 1/200 \cdot 1 = 1$$

or

$$\sigma_1 / \sigma_2 = 1/5000$$

which means that the tank conductivity scales up to  $2.4 \times 10^{-3}$  S/m (equivalent to a resistivity of 413 ohm m.).

The model transmitter loop is 1 m square, which scales up to 1 km square, and the model frequency range of 4 kHz to 400 kHz scales down to 20 Hz to 2000 Hz for the full-scale system.

This scaling therefore provides a typical frequency range for a Turam device, and it simulates a moderately conductive environment with a 413 ohm m ground.

### TURAM MODELLING RESULTS

The three examples presented here serve to demonstrate the ease with which the scale model can treat problems of exploration interest or investigate unusual operating procedures that may not easily be treated by mathematical modelling. An exhaustive report of all the information turned out by the system is not possible or appropriate here. Catalogues of the nonproprietary output of the modelling data will eventually be made available.

The first example illustrates a case in which the interaction between a conductive localized target structure and its moderately conductive host rock results in the gathering of current from the host rock into the target.

The target was a flat-lying tabular body at a simulated depth of 260 m, as shown in Figure 4. At the lowest frequency (50 Hz) the very mild anomaly in the RFSR profile of Figure 4 shows the characteristic positive and negative effects over the two edges of a flat-lying body, which indicate that this anomaly was due to direct induction of currents into the target.

At the higher frequencies both the RFSR and PD anomalies moved away from the transmitter to the extent that the PD anomaly displays its maximum 200 m away from the nearest edge of the body at 1000 Hz. This enhancement of the anomaly due to the gathering into the target of currents induced into the host rock has been reported by Gupta Sarma and Maru (1971) and by Gaur *et al.* (1972) for moving source devices, while the corresponding effect in Turam work was described by Lajoie and West (1976). These published studies, however, did not report the major displacements of Turam anomalies that appear to be possible in conductive environments, and that can clearly be very misleading in planning a drilling programme.

While the flat-lying target is not typical of many economic ore targets, it is similar in geometry to the elongated patches of highly conductive clay found near the base of the overburden of the Athabasca Basin of northern Saskatchewan. These results suggest that the gathering by these clays of current induced into the moderately conductive overburden may cause the clays to generate strong Turam anomalies, which could be mistaken for targets of economic interest.

A second problem not uncommon in Canadian exploration conditions is that of a steeply dipping, highly conductive target located in a very resistive host, but overlain by a moderately conductive overburden.

The possible consequences of interaction between overburden and target in this case are shown by Figure 5. Two examples are presented: in the first, the target and the overburden were not in electrical contact; in the second, they were connected and in the same positions. The anomalies shown at 50 Hz are identical in the two cases, hence we may infer that any currents induced into the overburden at this frequency were insignificant. An important feature of this anomaly is the fact that the positive peak lies over the lower edge of the target, because that edge was nearer to the transmitter than the upper edge. At 500 Hz the RFSR anomaly was stronger in both cases and the PD anomaly was weaker. This reduction of the PD anomaly was probably due to phase lag experienced by the primary field as it passed through the overburden. However, it appears that little disturbance of the induced current flow was taking place in either the target or the overburden. At 2000 Hz a further enhancement and inversion of the phase difference curve was seen in the case of no connection, but when overburden and target were connected, the curve showed a pronounced attenuation of the negative in the RFSR profile. This attenuation of the RFSR negative appears to have resulted from the

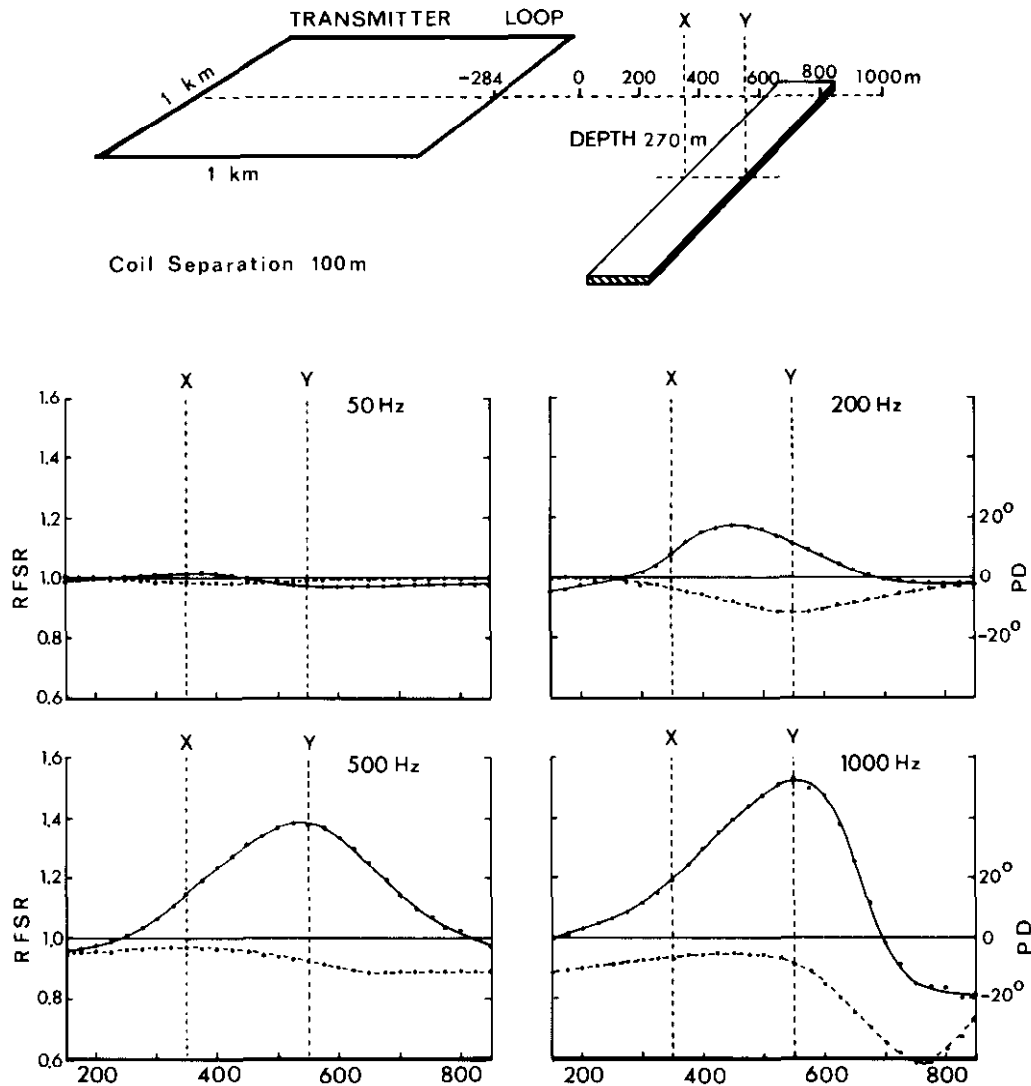
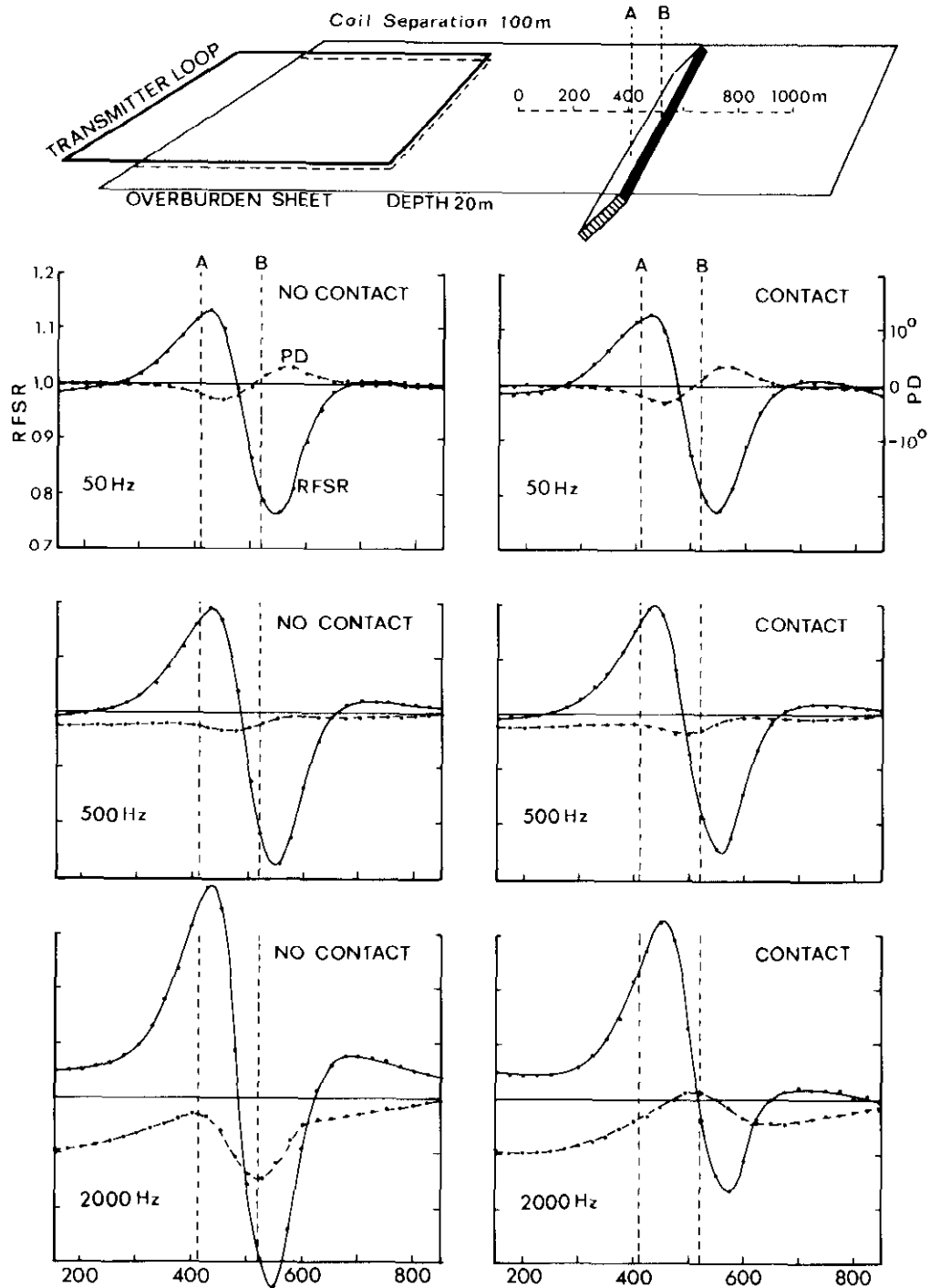


Fig. 4. Results of a conventional Turam modelling study over a flat-lying, tabular conductor ( $\sigma_c = 12.6 \text{ S/m}$ ) in a conductive host medium ( $\sigma_H = 2.4 \times 10^{-3} \text{ S/m}$ ). Solid curve depicts RFSR.

overburden having acted as a current source, which injected current into the target out of phase with the current induced directly into the target's top edge. It appears probable that if the target had dipped away from the transmitter, the directly induced currents in the top edge of the target would have been in phase with those induced into the overburden, in which case the galvanic connection of target and overburden would have resulted in an anomaly stronger than that for the nonconnected case. We have been unable to test this prediction because the tank would have to be returned to free space conditions, and we are reluctant to discard 21.6 tonnes of salt solution.

Even without confirmation of this prediction, it can be seen that conductive overburden can have a significant influence on the character of the anomaly due to a target, and that this effect will be difficult to predict because it depends on factors that cannot be known *a priori*.

The case of a target not in contact with the overburden was also treated for moving-source systems by Lowrie and West (1965), and for the Turam device by Lajoie and West (1976). In the Turam study the authors reported the phase rotation that is also evident in our results. However, in contrast to the anomaly enhancement we saw, they reported a general attenuation of the secondary field as the overburden conductivity was increased. A change of overburden conductivity was in effect simulated in our experiment by the change of frequency. Unfortunately, the increase of frequency also enhances the target response, so that these results cannot be directly compared with those of Lajoie and West (*ibid.*), and the anomaly enhancement that we report and the attenuation reported by those others are equally valid. We elected to study the change of frequency with a fixed model because of its correspondence to changes that the explorationist can make in the field survey.



**Fig. 5.** Results of a conventional Turam modelling study over a dipping, tabular conductor under a thin, conductive overburden sheet. (Dip 45°,  $\sigma_c = 12.6 \text{ S/m}$ .) Left-hand profiles show response with conductor and overburden electrically isolated. Right-hand profiles show response with conductor and overburden in galvanic contact.

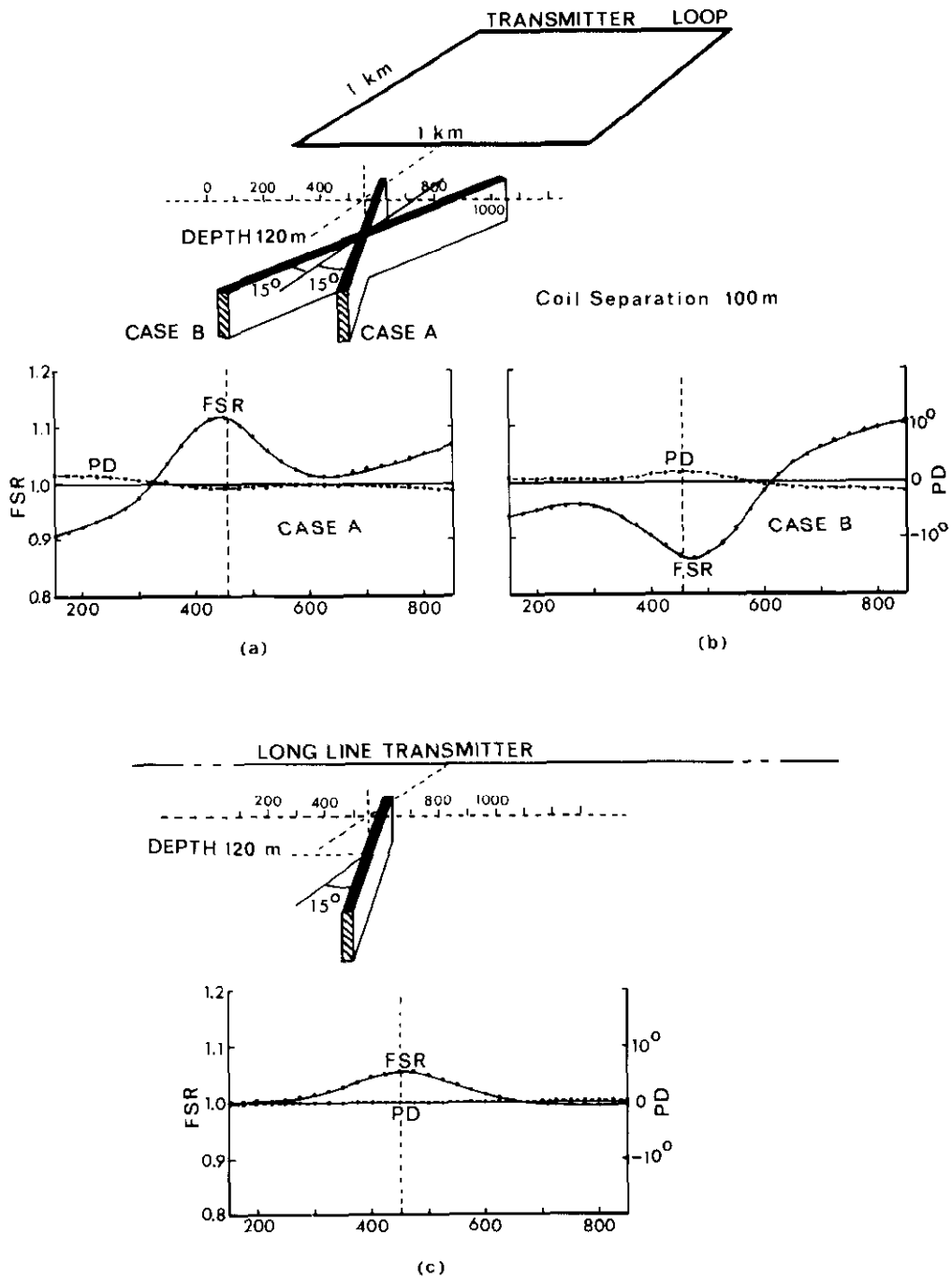


Fig. 6. Results of a Turam modelling study over a vertically dipping conductor ( $\sigma_c = 12.6$  S/m) using the alternative source configuration. Figs. 6a and 6b show the results obtained using a 1-km<sup>2</sup> loop source. Fig. 6c shows the results obtained with a long, ungrounded wire source.

The last example illustrates that the model can be used to investigate unconventional operating procedures that would present considerable difficulties in mathematical modelling.

The procedure that was the subject of this study is illustrated in Figure 6. It involves placing the front wire of the transmitter loop across the expected trend of a target, rather than parallel to it as in the normal procedure. Traverse lines are parallel to the side of the loop, and the receiver is operated in the normal manner along these lines. This arrangement immediately raises two questions: first, will targets lying at almost  $90^\circ$  with respect to the long axis of the transmitter loop be able to generate measurable anomalies, in view of their poor coupling with the transmitter field? second, even if detectable anomalies are generated, why would we want to use this procedure?

Only the model can answer the first question and the illustrations in Figure 6 show that it does so in the affirmative, indicating that a vertically dipping tabular body will generate significant anomalies at strike angles that deviate from  $90^\circ$  by as little as  $15^\circ$ . The reversal in response as the strike angle is changed from  $+15^\circ$  to  $-15^\circ$  with respect to perpendicular strike shows that, as may be expected, a position of perfect zero coupling exists for a  $90^\circ$  strike angle. Setting the model at exactly this zero point is difficult and no result for this condition is shown. A comparable test of the effect of dip showed similar behaviour, but changes of strike were found to be more important in the generation of anomalies.

Thus it seems probable that geologic reality will allow for significant coupling between transmitter and target, even with large angles of strike, and only extremely bad luck could allow a transmitter to be placed in perfect zero coupling with a real exploration target.

It therefore appears that the model results allow us to say that anomalies will be detectable in this mode of operation, but what is the intrinsic advantage? There are several, but the main one is that traverse length can be as long as required, depending only on loop length, whereas in normal Turam operations a 2-km line length is the maximum available, as it is controlled by transmitter power. This 2-km traverse length imposes an intrinsic limit of approximately 650 m on the depth at which normal Turam data can provide for detection and interpretation of an anomaly, because the features of an anomaly that must be considered for its full interpretation are distributed at surface over a traverse length at least three times the target depth.

An additional benefit is the freedom from strong primary field gradients along the traverse lines, which provides benefit in two ways. First, it eliminates the need to reduce field data to get rid of the primary gradient, as is necessary in normal Turam work. The

FSR profiles of Figures 6a and 6b were obtained by using a relatively small loop, so that a moderate gradient is visible in those data. When a long loop is used, as it was to obtain the profiles of Figure 6c, the primary gradient becomes negligible. The second benefit can be recognized when it is considered that the target shown in Figure 6c was immersed in a moderately conductive, uniform, host environment. This environment could not contribute any field gradient along the traverse, so that the system saw only the anomalous field due to the target. It would, of course, also see anomalies due to variations of conductivity within a nonuniform host, but it does appear that this procedure allows for the automatic rejection of the major effects due to conductive hosts or overburden layers.

Additional benefits appear to be possible and these will require future modelling studies. Among the possible benefits are the ability of this mode of operation to deal with closely grouped parallel conductors more effectively than can the normal mode of operation, and the possibility that it may allow Turam to be used more freely in a reconnaissance role. At this time we have some indications from both the model and the field trials that both these possibilities have merit, but more work is needed before the benefit can be fully established.

## CONCLUSIONS

We believe that this modelling facility is a significant addition to the capability for research that is available to the exploration industry. At present its output is of interest mainly to metallic-mineral explorationists, but we anticipate that developments in hand will make the system useful to the whole exploration industry.

## REFERENCES

- Bays, A.R. 1982, Development of an Electromagnetic Modelling Apparatus: M.Sc. thesis, University of Calgary, 148p.
- Boschart, R.A. 1964, Analytical Interpretation of Fixed Source Electromagnetic Prospecting Data: Ph.D. thesis, University of Delft, 102p.
- Gaur, V.K., Verma, O.P. and Gupta, C.P. 1972, Enhancement of electromagnetic anomalies by a conducting overburden: *Geophysical Prospecting*, v. 20, p. 580-604.
- Gupta, Sarma D. and Maru, V.M. 1971, A study of some effects of a conducting host rock with a new modelling apparatus: *Geophysics*, v. 36, p. 166-183.
- Lajoie, T.J. and West, G.F. 1976, The electromagnetic response of a conductive inhomogeneity in a layered earth: *Geophysics*, v. 41, p. 1133-1156.
- Lowrie, W. and West, G.F. 1965, The effect of a conducting overburden on electromagnetic prospecting measurements: *Geophysics*, v. 30, p. 624-632.
- Sinclair, G. 1948, Theory of models of electromagnetic systems: *Proc. IRE.*, v. 36, p. 1364-1370.